Anisotropic Skyrmion and Multi-q Spin Dynamics in Centrosymmetric Gd_2PdSi_3

M. Gomilšek,[1,2,3,*] T. J. Hicken,[4,3] M. N. Wilson,[5,3] K. J. A. Franke,[6,3] B. M. Huddart,[7,3] A. Štefančič,[8] S. J. R. Holt,[8,†] G. Balakrishnan,[8] D. A. Mayoh,[8] M. T. Birch,[9,10,3] S. H. Moody,[11,3] H. Luetkens,[4] Z. Guguchia,[4] M. T. F. Telling,[12] P. J. Baker,[12] S. J. Clark,[3] and T. Lancaster[3]

[1]*Jožef Stefan Institute, Jamova cesta 39, SI-1000 Ljubljana, Slovenia*
[2]*Faculty of Mathematics and Physics, University of Ljubljana, Jadranska ulica 19, SI-1000 Ljubljana, Slovenia*
[3]*Department of Physics, Durham University, South Road, Durham DH1 3LE, United Kingdom*
[4]*Laboratory for Muon Spin Spectroscopy, Paul Scherrer Institut, 5232 Villigen PSI, Switzerland*
[5]*Department of Physics and Physical Oceanography, Memorial University of Newfoundland, St. John's, NL A1B 3X7, Canada*
[6]*School of Physics and Astronomy, University of Leeds, Leeds LS2 9JT, United Kingdom*
[7]*Department of Physics, Clarendon Laboratory, University of Oxford, Oxford OX1 3PU, United Kingdom*
[8]*Department of Physics, University of Warwick, Coventry CV4 7AL, United Kingdom*
[9]*Max Planck Institute for Intelligent Systems, Heisenbergstrasse 3, D-70569 Stuttgart, Germany*
[10]*RIKEN Center for Emergent Matter Science, JP-351-0198 Wako, Japan*
[11]*Laboratory for Neutron Scattering and Imaging, Paul Scherrer Institut, 5232 Villigen PSI, Switzerland*
[12]*ISIS Facility, STFC Rutherford Appleton Laboratory, Didcot, Oxfordshire OX11 0QX, United Kingdom*

(Received 13 March 2024; revised 5 November 2024; accepted 11 December 2024; published 29 January 2025)

Skyrmions are particlelike vortices of magnetization with nontrivial topology, which are usually stabilized by Dzyaloshinskii-Moriya interactions (DMI) in noncentrosymmetric bulk materials. Exceptions are centrosymmetric Gd- and Eu-based skyrmion-lattice (SL) hosts with zero DMI, where both the SL stabilization mechanisms and magnetic ground states remain controversial. We address these here by investigating both the static and dynamical spin properties of the centrosymmetric SL host Gd_2PdSi_3 using muon spectroscopy. We find that spin fluctuations in the noncoplanar SL phase are highly anisotropic, implying that spin anisotropy plays a prominent role in stabilizing this phase. We also observe strongly anisotropic spin dynamics in the ground-state (IC-1) incommensurate magnetic phase of the material, indicating that it hosts a meronlike multi-q structure. In contrast, the higher-field, coplanar IC-2 phase is found to be single q with nearly isotropic spin dynamics.

DOI: 10.1103/PhysRevLett.134.046702

Topological spin textures can support exotic spin dynamics with a range of potential applications [1,2]. Especially promising are materials hosting skyrmions, which are topologically protected, noncoplanar vortices in the magnetization, that behave as extended particles [1,3]. While in bulk they are usually found in noncentrosymmetric materials and stabilized by Dzyaloshinskii-Moriya interactions (DMI), which select a skyrmion helicity [4], they were also found to be stabilized by competing magnetic interactions in bulk centrosymmetric compounds with no preferred helicity and no net DMI [1,2]. Examples are Gd_2PdSi_3, with a triangular spin lattice [5–15], $Gd_3Ru_4Al_{12}$ with a breathing kagome spin lattice [12,16–18], and $GdRu_2Si_2$ [19–28], $GdRu_2Ge_2$ [29], and $EuAl_4$ [30–32] with tetragonal spin lattices. Common to these highly symmetric rare-earth materials is that they host incommensurate skyrmion-lattice (SL) phases with very small (1.9–3.5 nm) skyrmions that are stable under higher applied fields (∼1 T) and over a wider range of T than their DMI-stabilized counterparts [1,2].

The stabilization mechanism for these centrosymmetric skyrmions is controversial, with suggestions including (i) short-range geometrical frustration [17,33–36], (ii) long-range Ruderman-Kittel-Kasuya-Yosida (RKKY) interactions plus dipolar [10,14,22,24,26,37] or biquadratic exchange [21,27,29,38–42], and (iii) competition of orbital-dependent exchange [43,44]. Most, but not all [38,39], such scenarios require spin anisotropy. The zero-field (ZF) ground state is also contentious [11], with early studies of Gd_2PdSi_3 suggesting an exotic, triple-q magnetic structure [5,6] [e.g., a lattice of merons and

*Contact author: matjaz.gomilsek@ijs.si

†Present address: Faculty of Engineering and Physical Sciences, University of Southampton, Southampton SO17 1BJ, United Kingdom and Max Planck Institute for the Structure and Dynamics of Matter, Luruper Chaussee 149, 22761 Hamburg, Germany.

antimerons (ML), which are half-skyrmion-like spin textures [21,25,29,45]], while recent calculations under scenario (ii) indicated a simpler, single-q helical ground state [10,37], as found in DMI-stabilized SL hosts [46]. Investigations of centrosymmetric SL hosts have focused on their static and topological properties, with less attention [32] paid to emergent spin dynamics [34], which can elucidate both the stabilization mechanisms and the single- or multi-q nature of their spin structures. Characteristic dynamics of SL and related spin textures have been observed in a range of DMI-stabilized SL hosts [1,2,47–49]. For accessing these, muon spectroscopy (μSR), a local-probe technique sensitive to spin fluctuations over a unique frequency range (applicable also at low applied fields and to conductive samples) [50], has proven valuable [51–57]. However, the narrow T range of DMI skyrmions [1,2,46] limited the ability to extract the underlying spin-wave dispersions unambiguously. Namely, when T is comparable to the transition temperature T_N, spin dynamics can become dominated by multimagnon processes and/or critical fluctuations (usually over $T_N/2 \lesssim T \lesssim 2T_N$), obscuring the underlying single-spin-wave dispersion.

In this Letter, we investigate the most-studied centrosymmetric SL host Gd_2PdSi_3 [5] using μSR and ac susceptibility, complemented by density functional theory (DFT) calculations of muon stopping sites [58]. We find clear signatures of spin reorientation transitions between the incommensurate magnetic phases and reveal the highly anisotropic character of their spin fluctuations. By exploiting the relatively wide region of stability of these phases, we characterize the low-energy dispersion relations of their spin-wave excitations. The excitations in the high-field coplanar incommensurate IC-2 phase are consistent with a single-q fanlike spin texture [5,6] with nearly isotropic spin fluctuations. However, in the ground-state ZF incommensurate IC-1 phase, we find that low-energy in-plane (ab-plane) spin fluctuations dominate, while out-of-plane (c-axis) fluctuations are almost completely suppressed. This, combined with previous resonant x-ray scattering (RXS) and resistivity data [5,6], indicates that the IC-1 phase is a complex, triple-q magnetic structure, not the recently predicted single-q helical structure [10,37]. This disfavors SL-stabilization scenario (ii) above. Finally, in the SL phase, out-of-plane fluctuations dominate instead, with in-plane fluctuations suppressed as a power law in T. We, therefore, argue that spin anisotropy is a key ingredient in stabilizing the SL phase in centrosymmetric rare-earth magnets.

Single crystals of Gd_2PdSi_3 were synthesized, with five high-quality $\approx 9\ \mathrm{mm}^2 \times 0.6$ mm platelike crystallites with c-axis normals extracted [15,58]. ac magnetic susceptibility measurements reproduced the phase diagram from previous studies [5–7], including the SL phase [Fig. 1(a)]. For μSR measurements, the crystallites were assembled in a mosaic with coaligned c axes [58]. The initial muon spin pointed

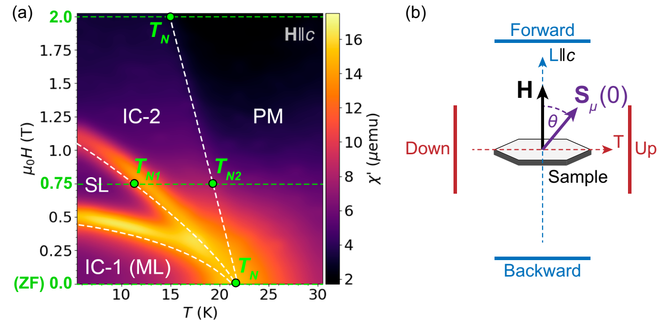

FIG. 1. (a) Real part of ac susceptibility with an applied field along the c axis. Phase boundaries (white) and μSR scans (green) with the corresponding transition temperatures T_N are shown. Phase assignments, including our suggested assignment of the IC-1 phase as a meron-antimeron lattice (ML), combine evidence from a range of experimental techniques [5–7]. (b) Sample and detector arrangement for μSR measurements. The initial muon spin $\mathbf{S}_\mu(0)$ lies at an angle θ to the applied field $\mathbf{H}\|c$, which points along the longitudinal direction L (blue). The transverse direction T (red) lies in the hexagonal ab plane.

along the out-of-plane (c-axis) direction in longitudinal-field (LF) measurements ($\theta = 0$), and at an angle of $\theta \approx 50°$ from the c axis in ZF and transverse-field (TF) measurements [Fig. 1(b)]. In a μSR experiment, longitudinal (L$\|c$) and transverse (T$\perp c$) muon spin components evolve independently [50], producing asymmetries $A_j(t) \propto \langle S_\mu^j(t)\rangle$ in detector pairs positioned along directions $j = \mathrm{L}$ and T [Fig. 1(b)], where $S_\mu^j(t)$ is the j-th component of muon spin $\mathbf{S}_\mu(t)$ at time t. An intermediate value of θ in ZF and TF experiments thus allowed us to track the different impacts of the material's magnetic state on the time evolution of the L and T muon spin components from a single experimental run. On the other hand, in LF experiments (where $\theta = 0$) only the L muon spin component could be measured. All measurements were made after first zero-field cooling the sample to base T, while magnetic fields were always applied along the c axis, which is an axis of threefold crystallographic symmetry, and thus a magnetic eigenaxis, of Gd_2PdSi_3.

We first performed μSR measurements on warming from the IC-1 ground state of Gd_2PdSi_3 in ZF on the GPS instrument at the Swiss Muon Source (SμS). At low T, a highly damped oscillation in the T-direction (ab-plane) muon spin component was observed at early times $t \ll 0.1$ μs [Fig. 2(a)] due to a broad distribution of quasistatic local fields at the muon site [58] that originate from long-range incommensurate magnetic ordering of Gd^{3+} spins. At later times, up to $t \approx 10$ μs, a further exponential relaxation was observed due to dynamical fluctuations of Gd^{3+} spins slower than the muon precession frequency [50]. The measured T-direction asymmetry data were fitted using $A(t) = [a_s - a_r]e^{-\sigma^2 t^2} + a_r e^{-\lambda t} + a_{\mathrm{bgd}}$, where $a_s = \mathrm{const.}$ is the total sample asymmetry and $a_{\mathrm{bgd}} = \mathrm{const.}$ is the background due to muons hitting the

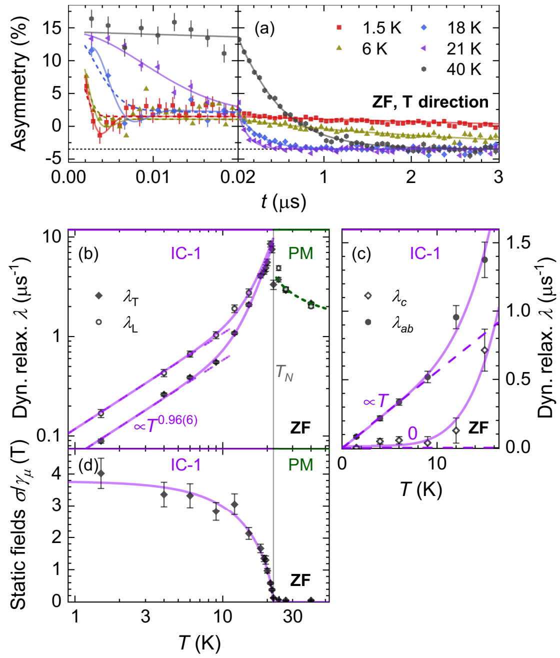

FIG. 2. IC-1 phase in ZF. (a) ab-plane (T-direction) muon asymmetry at early (left) and late times (right). Solid lines on the left-hand panel are guides to the eye; dashed lines are fits using the model described in the text. The horizontal dashed line shows the background level a_{bgd}. (b) Dynamical relaxation rates and (c) contributions to these rates due to out-of-plane (c-axis) and in-plane (ab-plane) spin fluctuations. Solid lines at $T < T_N$ are guides to the eye, which include a critical divergence near T_N (evident as an increase in λ above $\sim$10 K); dashed lines are the single-power-law low-T limits. (d) Strength of quasistatic magnetic fields extracted from fits of T-direction muon asymmetry.

sample holder. The early-time damping rate σ in this model is proportional to the average strength of quasistatic local magnetic fields at the muon site [58] and is expected to roughly scale with the magnitude of ordered moments in the sample. a_r is the late-time relaxing asymmetry due to the fraction of local fields that initially point along the measured muon spin component [58], and λ is the dynamical relaxation rate due to slow fluctuations of fields orthogonal to the measured muon spin component [50,58].

Fit results for the T direction are shown in Figs. 2(b) and 2(d) with the transition temperature $T_N = 22(1)$ K consistent with ac susceptibility [Fig. 1(a)]. In the itinerant paramagnetic (PM) regime at $T > T_N$ we find $\sigma \approx 0$. Around $T \approx T_N$, critical spin fluctuations cause λ_{T} to exhibit a divergence characteristic of a continuous phase transition as we enter the IC-1 phase. In the ordered IC-1 phase ($T < T_N$) the average local-field strength increases and saturates as an order parameter, $\sigma \propto [1 - (T/T_N)^{3/2}]^\beta$ [32,50] with $\beta = 0.7(1)$, which is large but close to $\beta = 0.50(5)$ found in the centrosymmetric SL host $EuAl_4$ in ZF [32]. At low T, slow spin fluctuations cross over into a power law $\lambda_{\mathrm{T}} \propto T^p$ with $p = 0.96(6)$. A low-T power-law dependence of the dynamical relaxation rate could be understood within spin-wave theory for a two-magnon process, which for a single gapless magnon band predicts [58–60]

$$p = \frac{2D}{s} - 1, \tag{1}$$

where $D \leq 3$ is the (integer) dimensionality of spin-wave excitations and s is the dominant power in their dispersion relation $\omega \propto |\mathbf{q} - \mathbf{q_0}|^s$ around the ordering wave vector $\mathbf{q_0}$. Usually, $s = 2$ for ferromagnetic ($\mathbf{q_0} = 0$) and $s = 1$ for antiferromagnetic and incommensurate states ($\mathbf{q_0} \neq 0$) [67]. The measured T-direction $p \approx 1$ in the IC-1 phase would thus correspond to a 1D (single-q) magnetic structure ($D = s = 1$), if the single-magnon-band approximation were valid.

To test this, we also fitted the L-direction (c-axis) data using the same model to obtain the relaxation rate λ_{L} [Fig. 2(b)]. Assuming bulk uniaxial symmetry around the c axis, we have [50,58] $\lambda_{\mathrm{L}} = 2\lambda_{ab}$ and $\lambda_{\mathrm{T}} = \lambda_{ab} + \lambda_c$, where λ_{ab} and λ_c are the relaxation rate contributions due to dynamical fluctuations of in-plane and out-of-plane magnetic fields at the muon site, respectively. At the nearly symmetric in-plane muon site that we obtain from DFT muon stopping site calculations (near the center of a Gd^{3+} triangle) [58], λ_{ab} and λ_c ultimately arise from fluctuations of in-plane and out-of-plane Gd^{3+} spin components, respectively. This can be seen from a symmetry decomposition of long-wavelength Gd^{3+} spin textures under local reflections over the ab-plane and rotations about the c-axis [for details, see the Supplemental Material (SM) [58]]. Figure 2(c) shows the extracted λ_{ab} and λ_c. Remarkably, in contrast to the single-magnon-band approximation where we should have $\lambda_{ab} \propto \lambda_c \propto T^p$ (for a proof, applicable also to general single-q states, see SM [58]), we instead find $\lambda_{ab} \propto T$ but $\lambda_c \approx 0$ in the IC-1 phase. Our first result is, therefore, that the IC-1 phase is not a simple single-q magnetic structure, as was predicted [10,37]. Instead, there appear to be multiple, highly anisotropic spin-fluctuation modes in this phase. Such behavior is expected for extended, multi-q spin textures [34,47], such as the hypothesized ML state [5,6]. Their predominantly in-plane nature appears consistent with easy-plane anisotropy found in this phase [11].

Next, we turn to the IC-2 and SL phases. Here, we performed separate μSR measurements in a TF of 0.75 T on the GPS instrument at SμS and an LF of 0.75 T on the HiFi instrument at the STFC-ISIS Facility. We warmed from the low-T SL to the intermediate IC-2 phase, and finally to the PM phase [Fig. 1(a)]. The late-time data were well described by the same model as for the ZF data, simplified to $A(t) = a_r e^{-\lambda t} + a_{\mathrm{bgd}}$ at late times. From T-direction TF data and L-direction LF data we again extracted in-plane λ_{ab} and out-of-plane λ_c spin-fluctuation contributions, as above.

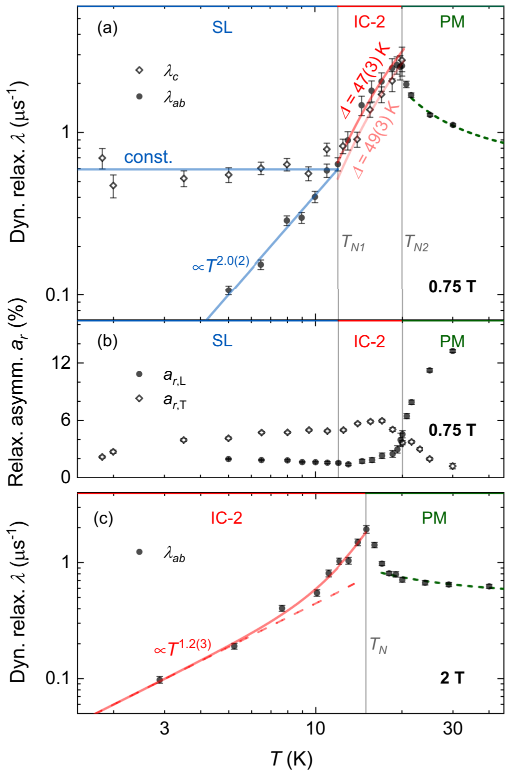

FIG. 3. (a) Contributions to relaxation due to out-of-plane (c-axis) and in-plane (ab-plane) spin fluctuations in the skyrmion-lattice (SL) and IC-2 phases in a 0.75 T applied field. (b) Relaxing asymmetry due to quasistatic local fields along the c axis (L) and within the ab plane (T) under these conditions. (c) Relaxation due to in-plane fluctuations in the IC-2 phase in a 2 T applied field.

The resulting relaxation rates are shown in Fig. 3(a) with transition temperatures $T_{N1} = 12(1)$ K and $T_{N2} = 20(1)$ K consistent with ac susceptibility [Fig. 1(a)]. The in-plane relaxation rate λ_{ab} shows a critical divergence at $T \approx T_{N2}$ due to a continuous transition between the PM and IC-2 phases. In the IC-2 regime ($T_{N1} < T < T_{N2}$) we find nearly isotropic spin fluctuations with $\lambda_c \approx \lambda_{ab}$. [Fitting these to a gapped model $\propto e^{-\Delta/T}$ also yields the same characteristic energy scales $\Delta = 47(3)$ and 49(3) K for λ_c and λ_{ab}, respectively.] Any low-T power-law spin-wave behavior is masked by near-critical fluctuations and interrupted by a transition to the SL phase at T_{N1}.

The phase transition at T_{N1} does not show any critical divergence in the muon relaxation rate, only a change of slope, implying that it is first order, consistent with the topologically nontrivial nature of the SL phase [1,34]. While nearly isotropic at T_{N1}, we find that highly anisotropic spin fluctuations emerge with lowering $T < T_{N1}$, similarly to the IC-1 phase. However, while in the IC-1 phase spin fluctuations were predominantly in plane ($\lambda_c \ll \lambda_{ab}$) the dominant spin fluctuations in the SL phase are instead out of plane, with $\lambda_c \approx$ const. $\gg \lambda_{ab} \propto T^p$ and $p = 2.0(2)$. We note that $p \approx 2$ would uniquely correspond to $D = 3$, $s = 2$ (3D ferromagnetic) spin excitations under the single-band spin-wave approximation [Eq. (1)], but this is inconsistent with a T-independent λ_c [58]. Instead, there appears to be a large low-energy spin density of states due to multiple spin fluctuation modes, as expected for SL phases [34,47–49,68], that are predominantly polarized out of plane (e.g., skyrmion breathing modes [47,68]).

We next turn to static properties of the SL and IC-2 phases in an applied field of 0.75 T. Figure 3(b) shows late-time relaxing asymmetries $a_{r,\mathrm{T}}$ and $a_{r,\mathrm{L}}$ in the in-plane (T) and out-of-plane (L) directions, respectively. Both change rather abruptly at $T \approx T_{N2}$ due to the onset of magnetic order. Assuming bulk uniaxial symmetry we expect [50,58] $a_{r,\mathrm{T}} \propto \langle \hat{B}_a^2 \rangle = \langle \hat{B}_b^2 \rangle$ and $a_{r,\mathrm{L}} \propto \langle \hat{B}_c^2 \rangle$, where $\hat{\mathbf{B}} = \mathbf{B}/|\mathbf{B}|$ is the initial direction of a quasistatic local field $\mathbf{B}$ at the muon site. In Fig. 3(b) we see that $a_{r,\mathrm{T}}$ exhibits a broad peak in the IC-2 phase at $T_{N1} < T < T_{N2}$, while $a_{r,\mathrm{L}}$ exhibits a minimum. These both indicate approximately coplanar quasistatic magnetism in this phase. In the SL phase, the difference between $a_{r,\mathrm{T}}$ and $a_{r,\mathrm{L}}$ becomes smaller, implying that local field directions become more isotropic, as expected for a noncoplanar spin texture [1–3]. Our observation of coplanar magnetism in the IC-2 phase and noncoplanar magnetism in the SL phase is consistent with RXS results [5], where this was argued based on the ellipticity of the magnetic moments of individual magnetic Bragg peaks. However, our conclusions are based on a complementary [11], real-space determination of local-field directions only accessible to local probes like the muon [50]. Intriguingly, via field-dependent quasistatic μSR measurements, we find that the width of the local field distribution does not scale with the average local-field strength in the SL phase, but does do so in the IC-1 and IC-2 phases (see the SM [58]).

Finally, to assess the low-T dynamics of the IC-2 phase, we performed μSR measurements in an LF of 2 T on the HiFi instrument. The late-time L-direction muon data were well described by the same model as for the 0.75 T data, where the fitted relaxation rate $\lambda_\mathrm{L} = 2\lambda_{ab}$ [Fig. 3(c)] shows a transition temperature $T_N = 15(1)$ K consistent with ac susceptibility [Fig. 1(a)]. Near $T \approx T_N$ the muon relaxation rate exhibits a critical divergence characteristic of a continuous phase transition as we enter the IC-2 phase, and at $T < T_N$ it crosses over into a low-T power law $\lambda_\mathrm{L} \propto T^p$ with $p = 1.2(3)$. The observed isotropy of spin fluctuations in this phase [Fig. 3(a)] makes single-band spin-wave theory [Eq. (1)] applicable, with the measured $p \approx 1$ indicating that the IC-2 phase is a 1D (single-q) magnetic structure ($D = s = 1$), as previously suggested [5,6]. This stands in contrast to multi-q IC-1 and SL phases found at lower applied fields.

To summarize, our finding of different low-T in-plane and out-of-plane spin fluctuations in both noncoplanar SL and ground-state IC-1 phases of centrosymmetric

Gd_2PdSi_3 contrasts with isotropic spin fluctuations found in the coplanar single-q IC-2 phase. This should supply a clue to the stabilization mechanism for centrosymmetric skyrmions. In contrast to DMI-stabilized skyrmions [47–49,68,69], systematic predictions for centrosymmetric SL spin dynamics for different stabilization mechanisms are lacking. Nevertheless, it seems unlikely that a spin model without strong intrinsic anisotropy could explain the observed highly anisotropic SL and IC-1 spin dynamics. This agrees with suggestions that spin anisotropy [11,34,42], combined with long-range interactions, is important for stabilizing the SL phase [10,17,27,40]. A quantitative determination of the anisotropy of intrinsic magnetic interactions in Gd_2PdSi_3 would thus be crucial [11]. We note that anisotropic magnetic interactions are also found in other representatives of the hexagonal R_2PdSi_3 family ($R =$ rare earth) [70,71], in the tetragonal centrosymmetric SL hosts $GdRu_2Si_2$ and $GdRu_2Ge_2$ [19,44,72–74], and even (weakly) in cubic Gd-based magnets [75]. Furthermore, our observation that the ground-state IC-1 phase is a multi-q magnetic structure (triple-q, based on previous RXS [5,6] and neutron-scattering [13] Bragg-peak studies) suggests it is the exotic ML state, as hypothesized in Ref. [5] from RXS and resistivity measurements. While double-q (square-lattice) ML-like states have recently been reported in thin-plate DMI-based $Co_8Zn_9Mn_3$ [45], and bulk tetragonal centrosymmetric $GdRu_2Ge_2$ [29] and $GdRu_2Si_2$ [21] (in two phases), the IC-1 phase would be a unique example of a triple-q magnetic ML. Furthermore, the IC-1 phase is the ZF ground state in Gd_2PdSi_3, while the ML states in $Co_8Zn_9Mn_3$ and $GdRu_2Ge_2$ are only stabilized under an applied field, and the claimed ZF ML phase in $GdRu_2Si_2$ has recently been reinterpreted as a topological-charge-stripe state instead [23,25,28]. The multi-q nature of the ZF IC-1 phase represents another challenge to theory, as calculations suggested that the ZF state should instead be single-q under the RKKY + dipolar skyrmion stabilization scenario (ii) [10,37]. Our findings thus disfavor this as the skyrmion stabilization mechanism. Nevertheless, RKKY interactions were found to be strong in the related centrosymmetric SL host $GdRu_2Si_2$ via angle-resolved photoemission spectroscopy (ARPES) [24,26] and quantum-oscillation measurements [22], complemented by *ab initio* calculations [21,22,24,26], so they could still play a role. A very recent ARPES and *ab initio* study of Gd_2PdSi_3 seems to support this [14].

In conclusion, in our muon-spectroscopy study of centrosymmetric Gd_2PdSi_3 we have found large anisotropy in spin dynamics, with qualitatively different behavior of dominant out-of-plane and subdominant in-plane spin fluctuations in the SL phase. We have also established the meronlike triple-q nature of its incommensurate IC-1 ground state with dominant in-plane, and nearly absent out-of-plane, spin fluctuations. The higher-field IC-2 phase was found to be coplanar and single-q with isotropic spin fluctuations. Our results suggest that the enigmatic stabilization mechanism behind SL phases in centrosymmetric Gd- and Eu-based materials is likely to be intimately related to spin anisotropy, and not solely RKKY + dipolar. Further local-probe studies of these and related centrosymmetric compounds [1,2,61,76] should be informative in exploring this. Studies of anisotropic spin excitations and their dispersions via inelastic neutron scattering [10], and the anisotropy of static spin correlations via RXS, especially on single crystals, would also be valuable. Finally, our μSR methods could also be extended to study low-T spin anisotropy and dynamics of metastable skyrmions in DMI-based SL hosts [1].

Acknowledgments—We thank Martin Klanjšek and Matej Pregelj at the Jožef Stefan Institute, Slovenia for helpful discussions. Parts of the work were carried out at the STFC ISIS Muon Source, United Kingdom and at the Swiss Muon Source, Paul Scherrer Institute, Switzerland and we are grateful for the provision of beam time and experimental support. We thank Raymond Fan and Paul Steadman for enabling us to use the Quantum Design MPMS3 at the I10 support laboratory, Diamond Light Source for ac susceptibility measurements. Computing resources were provided by the Durham HPC Hamilton cluster. M. G. acknowledges the financial support of the Slovenian Research and Innovation Agency through Program No. P1-0125 and Projects No. Z1-1852, No. N1-0148, No. J1-2461, No. J1-50008, No. J1-50012, No. N1-0345, and No. N1-0356. We acknowledge the financial support of the Engineering and Physical Sciences Research Council (EPSRC, UK) through Grants No. EP/N032128/1 and No. EP/N024028/1. The work at the University of Warwick was also funded by EPSRC, UK through Grant No. EP/T005963/1.

Data availability—Research data are available [77].

[1] S. Li, X. Wang, and T. Rasing, Magnetic skyrmions: Basic properties and potential applications, Interdiscip. Mater. **2**, 260 (2023).

[2] J. Khatua, B. Sana, A. Zorko, M. Gomilšek, K. Sethupathi, M. R. Rao, M. Baenitz, B. Schmidt, and P. Khuntia, Experimental signatures of quantum and topological states in frustrated magnetism, Phys. Rep. **1041**, 1 (2023).

[3] T. Lancaster, Skyrmions in magnetic materials, Contemp. Phys. **60**, 246 (2019).

[4] D. Morikawa, K. Shibata, N. Kanazawa, X. Z. Yu, and Y. Tokura, Crystal chirality and skyrmion helicity in MnSi and (Fe, Co)Si as determined by transmission electron microscopy, Phys. Rev. B **88**, 024408 (2013).

[5] T. Kurumaji, T. Nakajima, M. Hirschberger, A. Kikkawa, Y. Yamasaki, H. Sagayama, H. Nakao, Y. Taguchi, T. H. Arima, and Y. Tokura, Skyrmion lattice with a giant

topological Hall effect in a frustrated triangular-lattice magnet, Science **365**, 914 (2019).

[6] M. Hirschberger, T. Nakajima, M. Kriener, T. Kurumaji, L. Spitz, S. Gao, A. Kikkawa, Y. Yamasaki, H. Sagayama, H. Nakao, S. Ohira-Kawamura, Y. Taguchi, T. H. Arima, and Y. Tokura, High-field depinned phase and planar Hall effect in the skyrmion host Gd_2PdSi_3, Phys. Rev. B **101**, 220401(R) (2020).

[7] M. Hirschberger, L. Spitz, T. Nomoto, T. Kurumaji, S. Gao, J. Masell, T. Nakajima, A. Kikkawa, Y. Yamasaki, H. Sagayama, H. Nakao, Y. Taguchi, R. Arita, T. H. Arima, and Y. Tokura, Topological Nernst effect of the two-dimensional skyrmion lattice, Phys. Rev. Lett. **125**, 076602 (2020).

[8] H. Zhang, Q. Huang, L. Hao, J. Yang, K. Noordhoek, S. Pandey, H. Zhou, and J. Liu, Anomalous magnetoresistance in centrosymmetric skyrmion-lattice magnet Gd_2PdSi_3, New J. Phys. **22**, 083056 (2020).

[9] S. Spachmann, A. Elghandour, M. Frontzek, W. Löser, and R. Klingeler, Magnetoelastic coupling and phases in the skyrmion lattice magnet Gd_2PdSi_3 discovered by high-resolution dilatometry, Phys. Rev. B **103**, 184424 (2021).

[10] J. A. M. Paddison, B. K. Rai, A. F. May, S. Calder, M. B. Stone, M. D. Frontzek, and A. D. Christianson, Magnetic interactions of the centrosymmetric skyrmion material Gd_2PdSi_3, Phys. Rev. Lett. **129**, 137202 (2022).

[11] J. Ju, H. Saito, T. Kurumaji, M. Hirschberger, A. Kikkawa, Y. Taguchi, T. H. Arima, Y. Tokura, and T. Nakajima, Polarized neutron scattering study of the centrosymmetric skyrmion host material Gd_2PdSi_3, Phys. Rev. B **107**, 024405 (2023).

[12] K. K. Kolincio, M. Hirschberger, J. Masell, T. H. Arima, N. Nagaosa, and Y. Tokura, Kagome lattice promotes chiral spin fluctuations, Phys. Rev. Lett. **130**, 136701 (2023).

[13] T. Nakajima, H. Saito, N. Kobayashi, T. Kawasaki, T. Nakamura, H. Kawano-Furukawa, S. Asai, and T. Masuda, Polarized and unpolarized neutron scattering for magnetic materials at the triple-axis spectrometer PONTA in JRR-3, J. Phys. Soc. Jpn. **93**, 091002 (2024).

[14] Y. Dong, Y. Arai, K. Kuroda, M. Ochi, N. Tanaka, Y. Wan, M. D. Watson, T. K. Kim, C. Cacho, M. Hashimoto, D. Lu, Y. Aoki, T. D. Matsuda, and T. Kondo, Fermi surface nesting driving the RKKY interaction in the centrosymmetric skyrmion magnet Gd_2PdSi_3, Phys. Rev. Lett. **133**, 016401 (2024).

[15] D. Mayoh, A. Štefančič, M. Lees, and G. Balakrishnan, Crystal growth of the R_2PdSi_3 ($R =$ rare earth) materials using the optical floating zone technique, J. Cryst. Growth **642**, 127774 (2024).

[16] M. Hirschberger, T. Nakajima, S. Gao, L. Peng, A. Kikkawa, T. Kurumaji, M. Kriener, Y. Yamasaki, H. Sagayama, H. Nakao *et al.*, Skyrmion phase and competing magnetic orders on a breathing kagomé lattice, Nat. Commun. **10**, 5831 (2019).

[17] M. Hirschberger, S. Hayami, and Y. Tokura, Nanometric skyrmion lattice from anisotropic exchange interactions in a centrosymmetric host, New J. Phys. **23**, 023039 (2021).

[18] M. O. Ogunbunmi, H. S. Nair, and A. M. Strydom, Magnetic frustration-driven ground state properties of rare-earth magnetic ions on a breathing kagome lattice: a review of the $Gd_3Ru_4Al_{12}$ structure type magnets, Crit. Rev. Solid State Mater. Sci. **48**, 480 (2023).

[19] N. D. Khanh, T. Nakajima, X. Yu, S. Gao, K. Shibata, M. Hirschberger, Y. Yamasaki, H. Sagayama, H. Nakao, L. Peng *et al.*, Nanometric square skyrmion lattice in a centrosymmetric tetragonal magnet, Nat. Nanotechnol. **15**, 444 (2020).

[20] Y. Yasui, C. J. Butler, N. D. Khanh, S. Hayami, T. Nomoto, T. Hanaguri, Y. Motome, R. Arita, T. H. Arima, Y. Tokura *et al.*, Imaging the coupling between itinerant electrons and localised moments in the centrosymmetric skyrmion magnet $GdRu_2Si_2$, Nat. Commun. **11**, 5925 (2020).

[21] N. D. Khanh, T. Nakajima, S. Hayami, S. Gao, Y. Yamasaki, H. Sagayama, H. Nakao, R. Takagi, Y. Motome, Y. Tokura, T. H. Arima, and S. Seki, Zoology of multiple-Q spin textures in a centrosymmetric tetragonal magnet with itinerant electrons, Adv. Sci. **9**, 2105452 (2022).

[22] N. Matsuyama, T. Nomura, S. Imajo, T. Nomoto, R. Arita, K. Sudo, M. Kimata, N. D. Khanh, R. Takagi, Y. Tokura, S. Seki, K. Kindo, and Y. Kohama, Quantum oscillations in the centrosymmetric skyrmion-hosting magnet $GdRu_2Si_2$, Phys. Rev. B **107**, 104421 (2023).

[23] G. D. A. Wood, D. D. Khalyavin, D. A. Mayoh, J. Bouaziz, A. E. Hall, S. J. R. Holt, F. Orlandi, P. Manuel, S. Blügel, J. B. Staunton, O. A. Petrenko, M. R. Lees, and G. Balakrishnan, Double-Q ground state with topological charge stripes in the centrosymmetric skyrmion candidate $GdRu_2Si_2$, Phys. Rev. B **107**, L180402 (2023).

[24] S. Eremeev, D. Glazkova, G. Poelchen, A. Kraiker, K. Ali, A. Tarasov, S. Schulz, K. Kliemt, E. Chulkov, V. Stolyarov *et al.*, Insight into the electronic structure of the centrosymmetric skyrmion magnet $GdRu_2Si_2$, Nanoscale Adv. **5**, 6678 (2023).

[25] J. Spethmann, N. D. Khanh, H. Yoshimochi, R. Takagi, S. Hayami, Y. Motome, R. Wiesendanger, S. Seki, and K. von Bergmann, SP-STM study of the multi-Q phases in $GdRu_2Si_2$, Phys. Rev. Mater. **8**, 064404 (2024).

[26] Y. Dong, Y. Kinoshita, M. Ochi, R. Nakachi, R. Higashinaka, S. Hayami, Y. Wan, Y. Arai, S. Huh, M. Hashimoto *et al.*, Magnetic-domain-dependent pseudogap induced by Fermi surface nesting in a centrosymmetric skyrmion magnet, arXiv:2307.08000.

[27] J. A. Paddison, J. Bouaziz, A. F. May, Q. Zhang, S. Calder, D. Abernathy, J. B. Staunton, S. Blügel, and A. D. Christianson, Spin dynamics of the centrosymmetric skyrmion material $GdRu_2Si_2$, arXiv:2406.04524.

[28] B. Huddart, A. Hernández-Melián, G. Wood, D. Mayoh, M. Gomilšek, Z. Guguchia, C. Wang, S. Blundell, G. Balakrishnan, and T. Lancaster, Field-orientation-dependent magnetic phases in $GdRu_2Si_2$ probed with muon-spin spectroscopy, arXiv:2403.09431.

[29] H. Yoshimochi, R. Takagi, J. Ju, N. Khanh, H. Saito, H. Sagayama, H. Nakao, S. Itoh, Y. Tokura, T. Arima *et al.*, Multistep topological transitions among meron and skyrmion crystals in a centrosymmetric magnet, Nat. Phys. **20**, 1001 (2024).

[30] R. Takagi, N. Matsuyama, V. Ukleev, L. Yu, J. S. White, S. Francoual, J. R. Mardegan, S. Hayami, H. Saito, K. Kaneko *et al.*, Square and rhombic lattices of magnetic skyrmions in a centrosymmetric binary compound, Nat. Commun. **13**, 1472 (2022).

[31] T. Shang, Y. Xu, D. J. Gawryluk, J. Z. Ma, T. Shiroka, M. Shi, and E. Pomjakushina, Anomalous Hall resistivity and possible topological Hall effect in the $EuAl_4$ antiferromagnet, Phys. Rev. B **103**, L020405 (2021).

[32] X. Y. Zhu, H. Zhang, D. J. Gawryluk, Z. X. Zhen, B. C. Yu, S. L. Ju, W. Xie, D. M. Jiang, W. J. Cheng, Y. Xu, M. Shi, E. Pomjakushina, Q. F. Zhan, T. Shiroka, and T. Shang, Spin order and fluctuations in the $EuAl_4$ and $EuGa_4$ topological antiferromagnets: A μSR study, Phys. Rev. B **105**, 014423 (2022).

[33] T. Okubo, S. Chung, and H. Kawamura, Multiple-q states and the skyrmion lattice of the triangular-lattice Heisenberg antiferromagnet under magnetic fields, Phys. Rev. Lett. **108**, 017206 (2012).

[34] A. Leonov and M. Mostovoy, Multiply periodic states and isolated skyrmions in an anisotropic frustrated magnet, Nat. Commun. **6**, 8275 (2015).

[35] V. Lohani, C. Hickey, J. Masell, and A. Rosch, Quantum skyrmions in frustrated ferromagnets, Phys. Rev. X **9**, 041063 (2019).

[36] J. Pang, X. Niu, H. J. Zhao, Y. Zhang, and L. Bellaiche, Unravelling spontaneous Bloch-type skyrmion in centrosymmetric two-dimensional magnets, arXiv:2312.00423.

[37] J. Bouaziz, E. Mendive-Tapia, S. Blügel, and J. B. Staunton, Fermi-surface origin of skyrmion lattices in centrosymmetric rare-earth intermetallics, Phys. Rev. Lett. **128**, 157206 (2022).

[38] R. Ozawa, S. Hayami, and Y. Motome, Zero-field skyrmions with a high topological number in itinerant magnets, Phys. Rev. Lett. **118**, 147205 (2017).

[39] S. Hayami, R. Ozawa, and Y. Motome, Effective bilinear-biquadratic model for noncoplanar ordering in itinerant magnets, Phys. Rev. B **95**, 224424 (2017).

[40] S. Hayami and Y. Motome, Square skyrmion crystal in centrosymmetric itinerant magnets, Phys. Rev. B **103**, 024439 (2021).

[41] S. Hayami, Multiple skyrmion crystal phases by itinerant frustration in centrosymmetric tetragonal magnets, J. Phys. Soc. Jpn. **91**, 023705 (2022).

[42] S. Hayami, Anisotropic skyrmion crystal on a centrosymmetric square lattice under an in-plane magnetic field, J. Magn. Magn. Mater. **604**, 172293 (2024).

[43] T. Nomoto, T. Koretsune, and R. Arita, Formation mechanism of the helical $\boldsymbol{Q}$ structure in Gd-based skyrmion materials, Phys. Rev. Lett. **125**, 117204 (2020).

[44] T. Nomoto and R. Arita, *Ab initio* exploration of short-pitch skyrmion materials: Role of orbital frustration, J. Appl. Phys. **133**, 150901 (2023).

[45] X. Yu, W. Koshibae, Y. Tokunaga, K. Shibata, Y. Taguchi, N. Nagaosa, and Y. Tokura, Transformation between meron and skyrmion topological spin textures in a chiral magnet, Nature (London) **564**, 95 (2018).

[46] N. Kanazawa, S. Seki, and Y. Tokura, Noncentrosymmetric magnets hosting magnetic skyrmions, Adv. Mater. **29**, 1603227 (2017).

[47] M. Garst, J. Waizner, and D. Grundler, Collective spin excitations of helices and magnetic skyrmions: Review and perspectives of magnonics in non-centrosymmetric magnets, J. Phys. D **50**, 293002 (2017).

[48] T. Weber, D. M. Fobes, J. Waizner, P. Steffens, G. S. Tucker, M. Böhm, L. Beddrich, C. Franz, H. Gabold, R. Bewley *et al.*, Topological magnon band structure of emergent Landau levels in a skyrmion lattice, Science **375**, 1025 (2022).

[49] M. Soda, E. M. Forgan, E. Blackburn, E. Campillo, V. Ryukhtin, I. Hoffmann, A. Kikkawa, Y. Taguchi, H. Yoshizawa, and H. Kawano-Furukawa, Asymmetric slow dynamics of the skyrmion lattice in MnSi, Nat. Phys. **19**, 1476 (2023).

[50] S. J. Blundell, R. De Renzi, T. Lancaster, and F. L. Pratt, *Muon Spectroscopy: An Introduction* (Oxford University Press, Oxford, 2021).

[51] K. J. A. Franke, B. M. Huddart, T. J. Hicken, F. Xiao, S. J. Blundell, F. L. Pratt, M. Crisanti, J. A. T. Barker, S. J. Clark, A. Štefančič, M. C. Hatnean, G. Balakrishnan, and T. Lancaster, Magnetic phases of skyrmion-hosting $GaV_4S_{8-y}Se_y$ ($y = 0$, 2, 4, 8) probed with muon spectroscopy, Phys. Rev. B **98**, 054428 (2018).

[52] A. Štefančič, S. H. Moody, T. J. Hicken, M. T. Birch, G. Balakrishnan, S. A. Barnett, M. Crisanti, J. S. O. Evans, S. J. R. Holt, K. J. A. Franke, P. D. Hatton, B. M. Huddart, M. R. Lees, F. L. Pratt, C. C. Tang, M. N. Wilson, F. Xiao, and T. Lancaster, Origin of skyrmion lattice phase splitting in Zn-substituted Cu_2OSeO_3, Phys. Rev. Mater. **2**, 111402 (R) (2018).

[53] T. J. Hicken, S. J. R. Holt, K. J. A. Franke, Z. Hawkhead, A. Štefančič, M. N. Wilson, M. Gomilšek, B. M. Huddart, S. J. Clark, M. R. Lees, F. L. Pratt, S. J. Blundell, G. Balakrishnan, and T. Lancaster, Magnetism and Néel skyrmion dynamics in $GaV_4S_{8-y}Se_y$, Phys. Rev. Res. **2**, 032001(R) (2020).

[54] T. J. Hicken, M. N. Wilson, K. J. A. Franke, B. M. Huddart, Z. Hawkhead, M. Gomilšek, S. J. Clark, F. L. Pratt, A. Štefančič, A. E. Hall, M. Ciomaga Hatnean, G. Balakrishnan, and T. Lancaster, Megahertz dynamics in skyrmion systems probed with muon-spin relaxation, Phys. Rev. B **103**, 024428 (2021).

[55] M. N. Wilson, T. J. Hicken, M. Gomilšek, A. Štefančič, G. Balakrishnan, J. C. Loudon, A. C. Twitchett-Harrison, F. L. Pratt, M. Telling, and T. Lancaster, Spin dynamics in bulk MnNiGa and $Mn_{1.4}Pt_{0.9}Pd_{0.1}Sn$ investigated by muon spin relaxation, Phys. Rev. B **104**, 134414 (2021).

[56] T. J. Hicken, M. N. Wilson, S. J. R. Holt, R. Khassanov, M. R. Lees, R. Gupta, D. Das, G. Balakrishnan, and T. Lancaster, Magnetism in the Néel-skyrmion host GaV_4S_8 under pressure, Phys. Rev. B **105**, 134414 (2022).

[57] T. Hicken, M. Wilson, Z. Salman, T. Prokscha, A. Suter, F. Pratt, S. Zhang, G. van der Laan, T. Hesjedal, and T. Lancaster, Depth-dependent magnetic crossover in a room-temperature skyrmion-hosting multilayer, Phys. Rev. B **109**, 134423 (2024).

[58] See Supplemental Material at http://link.aps.org/supplemental/10.1103/PhysRevLett.134.046702 for details on crystal synthesis and characterization, ac susceptibility measurements, muon spectroscopy measurements (including field-dependent measurements), linear spin wave theory, *ab initio* (DFT) muon-site determination, and symmetry analysis of magnetic fields at the muon site, which includes Refs. [1,5–7,10,15,37,50,51,59–66].

[59] D. Beeman and P. Pincus, Nuclear spin-lattice relaxation in magnetic insulators, Phys. Rev. **166**, 359 (1968).

[60] N. Janša, A. Zorko, M. Gomilšek, M. Pregelj, K. W. Krämer, D. Biner, A. Biffin, C. Rüegg, and M. Klanjšek,

Observation of two types of fractional excitation in the Kitaev honeycomb magnet, Nat. Phys. **14**, 786 (2018).

[61] F. Tang, M. Frontzek, J. Dshemuchadse, T. Leisegang, M. Zschornak, R. Mietrach, J.-U. Hoffmann, W. Löser, S. Gemming, D. C. Meyer, and M. Loewenhaupt, Crystallographic superstructure in R_2PdSi$_3$ compounds ($R =$ heavy rare earth), Phys. Rev. B **84**, 104105 (2011).

[62] S. Toth and B. Lake, Linear spin wave theory for single-Q incommensurate magnetic structures, J. Phys. Condens. Matter **27**, 166002 (2015).

[63] B. Huddart, A. Hernández-Melián, T. Hicken, M. Gomilšek, Z. Hawkhead, S. Clark, F. Pratt, and T. Lancaster, MuFinder: A program to determine and analyse muon stopping sites, Comput. Phys. Commun. **280**, 108488 (2022).

[64] S. J. Clark, M. D. Segall, C. J. Pickard, P. J. Hasnip, M. J. Probert, K. Refson, and M. Payne, First principles methods using CASTEP, Z. Kristall. **220**, 567 (2005).

[65] J. P. Perdew, K. Burke, and M. Ernzerhof, Generalized gradient approximation made simple, Phys. Rev. Lett. **77**, 3865 (1996).

[66] H. J. Monkhorst and J. D. Pack, Special points for Brillouin-zone integrations, Phys. Rev. B **13**, 5188 (1976).

[67] J. Jensen and A. R. Mackintosh, *Rare Earth Magnetism: Structures and Excitations* (Oxford University Press, New York, 1991).

[68] M. Mochizuki, Spin-wave modes and their intense excitation effects in skyrmion crystals, Phys. Rev. Lett. **108**, 017601 (2012).

[69] X. Xing, Y. Zhou, and H. B. Braun, Magnetic skyrmion tubes as nonplanar magnonic waveguides, Phys. Rev. Appl. **13**, 034051 (2020).

[70] M. D. Frontzek, Magnetic properties of R_2PdSi$_3$ ($R =$ heavy rare earth) compounds, Ph.D. thesis, Technische Universität Dresden, Dresden, Germany, 2009, https://nbn-resolving.org/urn:nbn:de:bsz:14-qucosa-24779.

[71] M. Frontzek, A. Kreyssig, M. Doerr, M. Rotter, G. Behr, W. Löser, I. Mazilu, and M. Loewenhaupt, Magneto-crystalline anisotropy in R_2PdSi$_3$ ($R =$ Tb, Dy, Ho, Er, Tm) single crystals, J. Magn. Magn. Mater. **301**, 398 (2006).

[72] S. Sarkar, R. Pathak, A. Delin, O. Eriksson, and V. Borisov, Unveiling mysteries of GdRu$_2$Si$_2$: The impact of interlayer coupling on the magnetic response, arXiv:2409.06736.

[73] A. Garnier, D. Gignoux, D. Schmitt, and T. Shigeoka, Giant magnetic anisotropy in tetragonal GdRu$_2$Ge$_2$ and GdRu$_2$Si$_2$, Physica (Amsterdam) **222B**, 80 (1996).

[74] A. Garnier, D. Gignoux, N. Iwata, D. Schmitt, T. Shigeoka, and F. Zhang, Anisotropic metamagnetism in GdRu$_2$Si$_2$, J. Magn. Magn. Mater. **140**, 899 (1995).

[75] S. Jia, S. Bud'ko, G. Samolyuk, and P. Canfield, Nearly ferromagnetic Fermi-liquid behaviour in YFe$_2$Zn$_{20}$ and high-temperature ferromagnetism of GdFe$_2$Zn$_{20}$, Nat. Phys. **3**, 334 (2007).

[76] P. Kotsanidis, J. Yakinthos, and E. Gamari-Seale, Magnetic properties of the ternary rare earth silicides R$_2$PdSi$_3$ (R = Pr, Nd, Gd, Tb, Dy, Ho, Er, Tm and Y), J. Magn. Magn. Mater. **87**, 199 (1990).

[77] Data and computer code from this paper can be found at 10.6084/m9.figshare.28024910.v1.